AGU ADVANCING EARTH AND SPACE SCIENCE

Geophysical Research Letters

RESEARCH LETTER
10.1029/2022GL102546

Reduced Tropical Climate Land Area Under Global Warming

Ori Adam[1], Noga Liberty-Levi[1], Michael Byrne[2,3], and Thomas Birner[4]

[1]The Fredy and Nadine Herrmann Institute of Earth Sciences, The Hebrew University, Jerusalem, Israel, [2]School of Earth and Environmental Sciences, University of St Andrews, St Andrews, UK, [3]Department of Physics, University of Oxford, Oxford, UK, [4]Meteorologisches Institut, Ludwig-Maximilians-Universität, Munich, Germany

Key Points:

- Net tropical climate land area, defined by smaller seasonal than diurnal temperature range, is projected to decrease in a warming climate
- The decrease is primarily due to enhanced summer warming, leading to an elevated seasonal temperature range in the tropics
- The decrease agrees with narrowing of the tropical rain belt and expansion of the subtropical dry zone at its equatorward and poleward sides

Supporting Information:

Supporting Information may be found in the online version of this article.

Correspondence to:

O. Adam,
ori.adam@mail.huji.ac.il

Citation:

Adam, O., Liberty-Levi, N., Byrne, M., & Birner, T. (2023). Reduced tropical climate land area under global warming. *Geophysical Research Letters*, *50*, e2022GL102546. https://doi.org/10.1029/2022GL102546

Received 14 DEC 2022
Accepted 3 MAR 2023

Author Contributions:

Data curation: Noga Liberty-Levi
Methodology: Noga Liberty-Levi

Abstract

Regions along the edges of the tropics host vast populations and ecosystems which are sensitive to climate change. Here we examine the extent of tropical land areas in the ERA5 and MERRA-2 reanalyses and in high-emission scenarios of 45 models participating in phases 5 and 6 of the Coupled Model Intercomparison Project (CMIP5/6). Based on the definition of tropical climate land areas as regions where the diurnal temperature range exceeds the seasonal temperature range, we find a net reduction of tropical land area with global warming. This change is primarily due to an increased seasonal temperature range driven by enhanced summer warming, which in turn is largely driven by reduced evaporative cooling. The reduction of tropical climate area is consistent with a narrowing of the tropical rain belt and with an equatorward and poleward expansion of the subtropical dry zones. Understanding the links between these trends requires further study.

Plain Language Summary

Tropical climate land areas host about 40% of the world's population and 80% of the world's biodiversity. Changes in the extent of tropical climate land areas, which generally border semi-arid climate zones, can therefore carry vast ecological and socio-economic implications. Tropical climate land areas are generally defined as regions where the daily temperature range exceeds the seasonal temperature range. Based on this definition we find a net decrease in tropical climate land area in climate model projections of greenhouse-gas-induced global warming. The net reduction in tropical land area is driven primarily by increased seasonal temperature range, due to enhanced summer warming, which in turn is largely driven by drying. The reduction in tropical climate land area in a warming climate agrees with a narrowing of the tropical rain belt and with "Subtropical widening", that is, a poleward and equatorward expansion of the subtropical dry zones. However, understanding the links between these trends requires further study.

1. Introduction

Tropical climate land areas host about 40% of the world's population and 80% of the world's biodiversity (Gaston, 2000; Lehner & Stocker, 2015; Warszawski et al., 2017). Changes in the extent of tropical climate land areas, which generally border semi-arid climate zones, can therefore carry vast ecological and socio-economic implications (Barlow et al., 2018; Grünzweig et al., 2022; Ruane et al., 2021). Tropical climate land areas may be affected by various changes driven by global warming, which include the expansion of the tropical meridional overturning circulation (MOC) and subtropical dry zones (SDZs) (Lu et al., 2007; Seidel et al., 2008; Staten et al., 2020), the expansion of global drylands (Feng & Fu, 2013; Fu & Feng, 2014; Huang et al., 2017; Sherwood & Fu, 2014), increased monsoonal variability (B. Wang et al., 2021), as well as narrowing and regional shifts of the tropical rain belt (TRB) (Byrne & Schneider, 2016b; Liu et al., 2022; Mamalakis et al., 2021). It is therefore important to assess the response of tropical land areas to global warming and to understand its relation to global trends. Here we analyze projected changes under global warming in the extent of tropical climate land areas using a simple definition of tropical zones based on temperature variations, and relate these changes to trends in the SDZs and the TRB.

In the present climate, seasonal temperature variations nearly vanish near the equator and generally increase toward the poles—in accordance with seasonal insolation (Riehl, 1979). Diurnal temperature variations are similarly lower near the equator but vary modestly between tropical and subtropical latitudes (Riehl, 1979; Yang & Slingo, 2001). In addition, owing to the large difference in heat capacity, tropical surface temperature variations over land are larger than over ocean by factors of about 10 and 2 on diurnal and seasonal timescales, respectively, making diurnal surface temperature variations significantly larger than seasonal variations in the tropics (Riehl, 1954, 1979). Tropical climate land areas are therefore conveniently defined as land regions where the

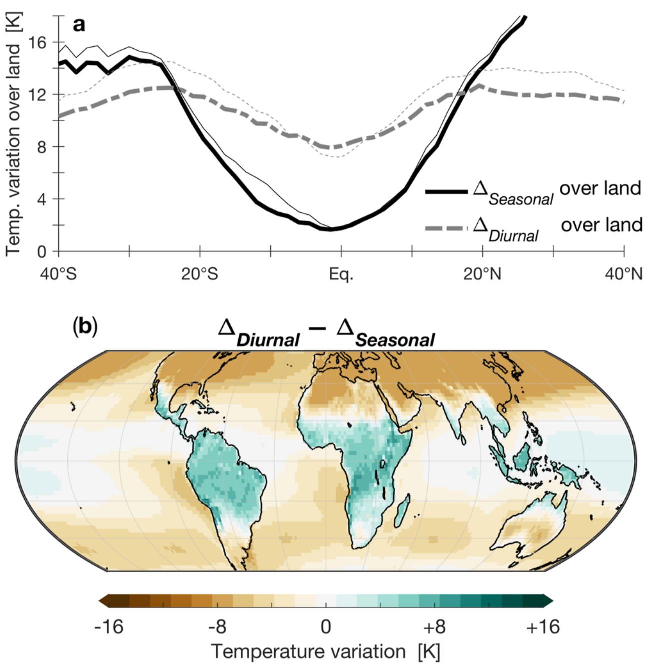

Figure 1. (a) Seasonal (solid black) and diurnal (dashed gray) surface temperature ranges ($\Delta_{Seasonal}$ and $\Delta_{Diurnal}$, respectively), zonally averaged over land areas. (b) Global $\Delta_{Diurnal} - \Delta_{Seasonal}$. Data shown for climatological values of the European Centre for Medium-Range Weather Forecasts ERA5 data set (panel (b) and thick lines in panel (a), Hersbach et al., 2020), and for the National Aeronautics and Space Administration MERRA-2 data set (thin lines in panel (a), Gelaro et al., 2017), for the years 1980–2020. See Section 2 for details on the data and calculations.

diurnal temperature range exceeds the seasonal temperature range—a definition commonly attributed to Riehl (1979), but first proposed by Troll (1943) and demonstrated by Paffen (1967).

Figure 1 shows the observed climatological mean differences over land between maximal and minimal diurnal surface air temperatures ($\Delta_{Diurnal}$) and between the hottest and coldest months in each year ($\Delta_{Seasonal}$). Tropical climate land areas, where $\Delta_{Diurnal} > \Delta_{Seasonal}$, are clearly delineated from subtropical areas, with mean edges at about 24° S and 17° N. Changes associated with global warming in the extent of tropical land areas, as defined above, thus depend on the responses of seasonal and diurnal surface temperature variations.

The sensitivities of seasonal and diurnal temperature variability to global warming have been extensively analyzed in modeling and observational studies (e.g., Chen et al., 2019; Donohoe & Battisti, 2013; Dwyer et al., 2012; Holmes et al., 2016; Manabe et al., 2011; Sobel & Camargo, 2011; Stine & Huybers, 2012; Stouffer & Wetherald, 2007; Yettella & England, 2018). At high latitudes, the seasonal temperature range generally decreases with global warming due to enhanced winter warming (e.g., Chen et al., 2019; Dwyer et al., 2012; Manabe et al., 2011). The diurnal temperature range has likewise generally decreased globally over the past century, especially at higher latitudes, due to enhanced nighttime warming (Thorne, Donat, et al., 2016; Thorne, Menne, et al., 2016; K. Wang & Clow, 2020; Wild, 2009).

In contrast, at low latitudes global warming is associated with a weak general increase in both seasonal and diurnal surface temperature variability. The increase in the seasonal temperature range is mainly attributed to reduced evaporative cooling during summer, caused by decreased relative humidity and weakened circulation (Chen et al., 2019; Sobel & Camargo, 2011). The diurnal temperature range is generally lower during summer, and therefore affected by the elevated summer temperatures (Geerts, 2003; Yang & Slingo, 2001). However, both seasonal and diurnal temperature variations over land depend strongly on local processes which are typically not well simulated by climate models. There is therefore generally poor consistency across climate models and between observed and projected changes in both seasonal and diurnal tropical temperature variations, especially at regional scales (Chen et al., 2019; Dwyer et al., 2012; Thorne, Donat, et al., 2016; C. Wang et al., 2014; K. Wang & Clow, 2020; Yin & Porporato, 2017).

Here we use the temperature-range definition of tropical climate land areas to examine the extent of tropical land areas in reanalyses and in projections by coupled climate models. Our methodology is described in Section 2, followed by our results and a summary and discussion in Sections 3 and 4.

2. Data and Methods

Observationally constrained data is taken from the European Center for Medium-Range Weather Forecasts (ECMWF) ERA5 reanalysis (0.25° × 0.25° resolution; Hersbach et al., 2020), and from the National Aeronautics and Space Administration MERRA-2 reanalysis (0.625° × 0.5°; Gelaro et al., 2017) for the years 1980–2020.

The seasonal and diurnal temperature ranges are calculated using 2m surface air temperature. The seasonal temperature range ($\Delta_{Seasonal}$) is calculated as the difference between the warmest and coldest individual months in each year at each grid cell. The diurnal temperature range ($\Delta_{Diurnal}$) is calculated as the annual mean difference between monthly maximal and minimal diurnal temperatures at each grid cell, derived from hourly data. We derive two parameters from the difference between $\Delta_{Diurnal}$ and $\Delta_{Seasonal}$: (a) Tropical land width is calculated as the distance between the northern and southern latitudes where $\Delta_{Diurnal} - \Delta_{Seasonal}$ changes sign; (b) Tropical land area is calculated as the area-weighted sum over all land grid cells in which $\Delta_{Diurnal} > \Delta_{Seasonal}$. The land mask includes all areas with less than 10% surface water or ice (e.g., Pekel et al., 2016), which excludes large lakes (e.g., lake Chad in central Africa). For reference, the climatologies of observed seasonal and diurnal surface

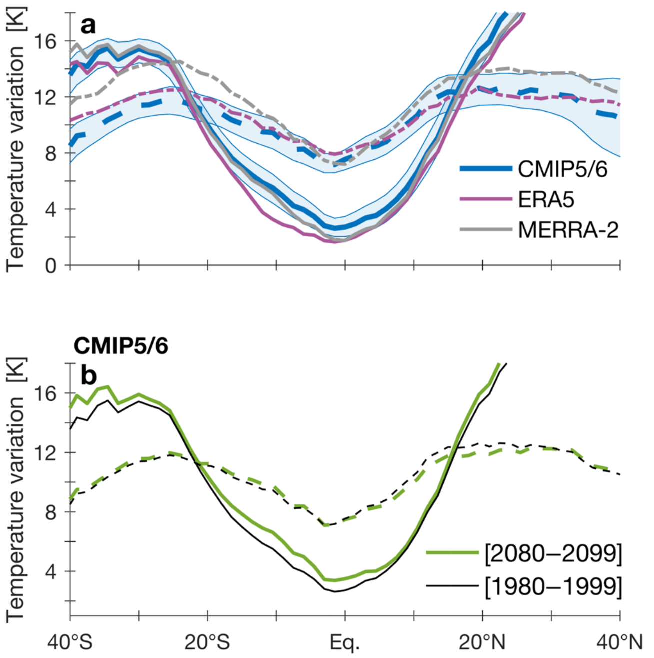

Figure 2. (a) Seasonal ($\Delta_{Seasonal}$, solid) and diurnal ($\Delta_{Diurnal}$, dashed) surface temperature ranges, zonally averaged over land, for CMIP5/6 historical simulations (blue) and for the ERA5 (purple) and MERRA-2 (gray) reanalyses. Shading indicates ±1 standard deviation across models. (b) Ensemble mean CMIP5/6 values of $\Delta_{Seasonal}$ (solid) and $\Delta_{Diurnal}$ (dashed), zonally averaged over land, for the periods 1980–1999 (black, historical simulations) and 2080–2099 (green, RCP85/SSP585 simulations).

temperature ranges are shown and discussed in the Supporting Information (Figure S1 in Supporting Information S1).

We also analyze tropical temperature variations in 27 climate models from Phase 5 (Taylor et al., 2012) and 18 models from Phase 6 (Eyring et al., 2016) of the Coupled Model Intercomparison Project (CMIP5/6), based on availability (Table S1 in Supporting Information S1). For CMIP5/6 models, $\Delta_{Seasonal}$ is calculated from monthly surface air temperature fields (i.e., the "tas" variable), and $\Delta_{Diurnal}$ is calculated as the annual mean difference between monthly maximal and minimal daily surface temperatures at each grid cell (i.e., using the "tasmax" and "tasmin" variables). For each model we use data only from the first realization (ensemble members "r1i1p1" and "r1i1p1f1" for CMIP5 and CMIP6, respectively), linearly interpolated to a common 1.5° × 1.5° horizontal grid.

To examine the relation of tropical land areas to the SDZs, we analyze variations in precipitation minus evaporation ($P - E$) in the 27 CMIP5 models and in 16 of the 18 CMIP6 models ($P - E$ data is not available for the "GFDL-ESM4" and "CAS-ESM2-0" models; see Table S1 in Supporting Information S1). Specifically, the extent of the SDZs increases with global warming, and is known to strongly covary with the width of the tropical MOC (Lu et al., 2007; Seviour et al., 2018). We calculate the equatorward and poleward extents of the SDZs as the subtropical latitudes where the zonal mean $P - E$ (over land and ocean) changes from positive to negative and from negative to positive, respectively, averaged over the northern and southern hemispheres, using the TropD software package (Adam et al., 2018) (Note that this definition cannot be applied to only land areas, because evaporation nearly vanishes over land). We also analyze the width of the tropical rain belt (TRB, or the width of the intertropical convergence zone), which is projected to decrease under global warming (Byrne & Schneider, 2016b). The width of the TRB is calculated as the standard deviation of the meridional distribution of precipitation equatorward of 20°, which is well correlated with other indices of the TRB width (Adam et al., 2023, see the Appendix for details). We apply this definition to the zonal mean precipitation (over land and ocean), as well as to precipitation zonally averaged over land.

To gauge model biases, we compare historical simulations averaged over the period 1980–1999 with the ERA5 and MERRA-2 reanalyses. For assessing the sensitivity to global warming, we take the averaged difference between years 2080–2099 in the RCP85 (CMIP5) and SSP585 (CMIP6) scenarios, in which pre-industrial CO_2 levels are quadrupled by the end of the 21st century, and the historical simulations. As shown in Figure S2 in Supporting Information S1, the zonally land-averaged representation of $\Delta_{Seasonal}$ and $\Delta_{Diurnal}$ in the two CMIP phases is statistically indistinguishable; we therefore analyze the two phases jointly. We note that CMIP5/6 models are known to have regional biases in precipitation (Fiedler et al., 2020) and seasonal temperature variability, mainly associated with coupled large-scale circulation (Chen et al., 2019; C. Wang et al., 2014), as well as deficiencies in the representation of diurnal temperature variations, associated with biases in cloud, surface, and vegetation processes (K. Wang & Clow, 2020; Yin & Porporato, 2017).

3. Results

3.1. Zonal Mean Trends

Figure 2a compares $\Delta_{Seasonal}$ and $\Delta_{Diurnal}$ in the CMIP5/6 historical simulations and in the ERA5 and MERRA-2 datasets, zonally averaged over land. In the subtropical latitudes where $\Delta_{Diurnal} - \Delta_{Seasonal}$ changes sign, the model seasonal temperature ranges are in broad agreement with the reanalyzes. However, diurnal temperature ranges do not agree across both models and reanalyses, for example, in the southern hemisphere where the models underestimate $\Delta_{Diurnal}$ (more so when compared with MERRA-2), reflecting the large uncertainty in simulating diurnal temperature variations (K. Wang & Clow, 2020). Given the discrepancies across reanalyzes and the significant

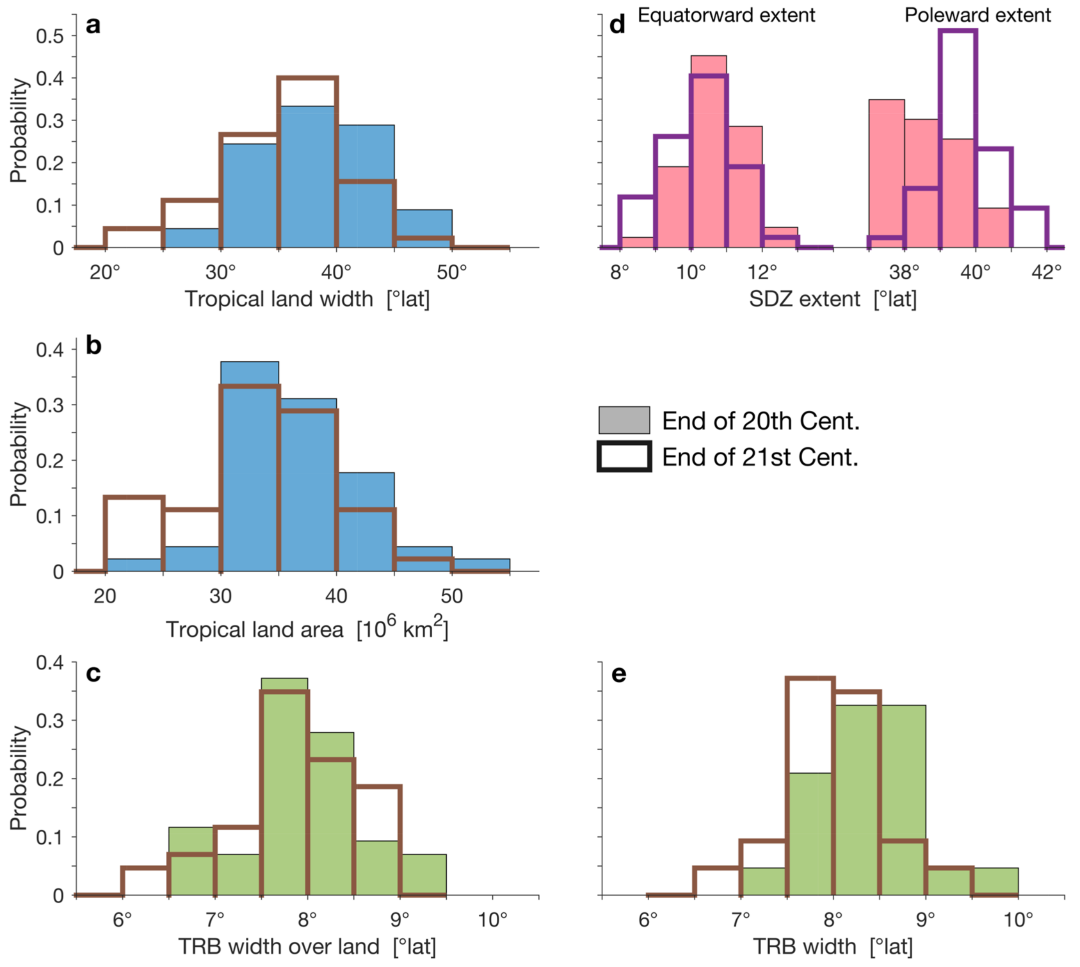

Figure 3. CMIP5/6 models probability distribution functions (PDFs) of (a) tropical land width (mean latitudinal extent of land where $\Delta_{\mathrm{Diurnal}} > \Delta_{\mathrm{Seasonal}}$), (b) tropical land area (net land area where $\Delta_{\mathrm{Diurnal}} > \Delta_{\mathrm{Seasonal}}$), (c) width of the tropical rain belt (TRB) over land, (d) the equatorward and poleward extents of the subtropical dry zones (SDZs), and (e) width of the TRB over land and ocean. End of 20th century (historical simulations) and end of 21st century values (RCP85/SSP585 simulations) are shown in colored bars and thick frames, respectively. Note that left and right panels are averaged over land and ocean + land, respectively, and that values in panel d are averaged over both hemispheres. The PDFs are composed of 45 models in panels (a) and (b), and of 43 models in panels (c–e).

role of natural variability in observed tropical widening trends (Adam et al., 2014; Nguyen et al., 2013; Staten et al., 2018), our analysis hereon focuses only on long-term trends associated with global warming in CMIP5/6 projections. The large inter-model variance introduces uncertainty in projections of both $\Delta_{\mathrm{Seasonal}}$ and $\Delta_{\mathrm{Diurnal}}$. Nevertheless, simulated ensemble-mean trends have been shown to be consistent with observed trends in recent decades of both $\Delta_{\mathrm{Seasonal}}$ (Chen et al., 2019) and $\Delta_{\mathrm{Diurnal}}$ (K. Wang & Clow, 2020), which provides some confidence in the projected mean trends.

Figure 2b shows the CMIP5/6 ensemble means of $\Delta_{\mathrm{Seasonal}}$ and $\Delta_{\mathrm{Diurnal}}$, zonally averaged over land, in historical simulations and in projections. Consistent with previous analyses, a general increase in tropical $\Delta_{\mathrm{Seasonal}}$ is seen, due to enhanced warming during the warm season (e.g., Chen et al., 2019). $\Delta_{\mathrm{Diurnal}}$ decreases in the northern hemisphere and slightly increases in the southern hemisphere. These changes are driven by cloud radiative effects, precipitation, and surface heat fluxes, which vary across regions (Dai et al., 1997; K. Wang & Clow, 2020). Overall, the changes in $\Delta_{\mathrm{Seasonal}}$ and $\Delta_{\mathrm{Diurnal}}$ suggest a net decrease in the extent of tropical land area.

Indeed, Figures 3a and 3b shows model probability distribution functions (PDFs) of tropical land width (mean latitudinal extent of land where $\Delta_{\mathrm{Diurnal}} > \Delta_{\mathrm{Seasonal}}$) and of tropical land area (net land area where $\Delta_{\mathrm{Diurnal}} > \Delta_{\mathrm{Seasonal}}$) for the ends of the 20th and 21st centuries. A shift toward reduced tropical width and area is seen in nearly

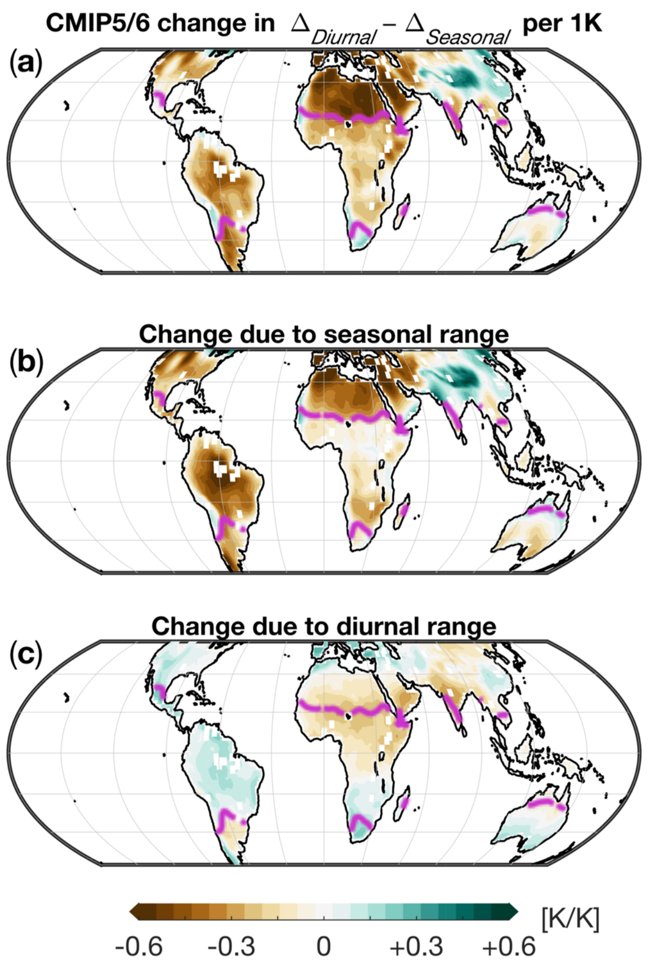

Figure 4. CMIP5/6 ensemble mean change in $\Delta_{\text{Diurnal}} - \Delta_{\text{Seasonal}}$ per 1K global mean temperature warming. (a) Total change; (b) change due to Δ_{Seasonal} (i.e., Δ_{Diurnal} is held fixed); (c) change due to Δ_{Diurnal} (i.e., Δ_{Seasonal} is held fixed). Magenta lines show latitudes where $\Delta_{\text{Diurnal}} - \Delta_{\text{Seasonal}} = 0$. Positive (negative) values indicate transition toward tropical (semi-arid) climate.

all of the models, indicating a reduced net tropical extent under global warming (ensemble mean decrease in width and area per 1K is 0.48° and 0.78×10^6 km^2; see Figure S3 and Table S2 in Supporting Information S1 for PDFs and statistical parameters of the projected changes per 1K global warming).

The expansion of the SDZs along the descending branches of the tropical mean MOC, commonly termed "Tropical widening" (e.g., Staten et al., 2020), is often considered as a possible driver of regional climatic changes (e.g., D'Agostino & Lionello, 2020; Garfinkel et al., 2020; Seager et al., 2010, 2014; Si et al., 2009; Tuel et al., 2021). We therefore next examine the relation of projected changes in the SDZs and the TRB to those in tropical land extent. Changes in the equatorward and poleward extents of the SDZs are shown in Figure 3d, indicating an equatorward and poleward expansion of the SDZs (e.g., Byrne & Schneider, 2016a; Seviour et al., 2018; Waugh et al., 2018). Consistent with the equatorward expansion of the SDZs, the width of the zonal mean TRB (Figure 3e), which follows the width of the rising branch of the MOC, decreases (Byrne & Schneider, 2016b). However, as shown in Figure 3d, there is no clear change in the width of the TRB over land. The narrowing of tropical climate land area is therefore consistent with but not clearly related to the expansion of the SDZs (or narrowing of the TRB), which are attributed to changes in the tropical MOC, but are manifested primarily over ocean due to confounding effects by land-ocean temperature contrast and radiative forcing (He & Soden, 2017; Schmidt & Grise, 2017).

3.2. Regional Trends

We now turn to examine regional changes. Given the similarities between the width and area indices, and given that tropical zonally varying width is not well defined in narrow continent strips (Figure 1b), we focus our regional analysis on tropical land area.

Figure 4a shows the projected ensemble-mean changes per 1K warming in $\Delta_{\text{Diurnal}} - \Delta_{\text{Seasonal}}$. Reduction of tropical land area is seen over Africa and the Americas in most models (model agreement is about 70% along the boundaries of the tropical climate land areas), and to a lesser degree over the Asian and western Pacific sectors (see Figures S4 and S5 in Supporting Information S1 for PDFs of the regional changes and model agreement). Specifically, the ensemble-mean projected regional changes in tropical land area per 1K are -0.31×10^6 km^2 over Africa, -0.43×10^6 km^2 over the Americas, and -0.03×10^6 km^2 over Asia and the western Pacific sectors.

The particular contributions of changes in Δ_{Seasonal} and Δ_{Diurnal} are shown in Figures 4b and 4c. Most of the reduction in net tropical land area is due to increased Δ_{Seasonal}, with Δ_{Diurnal} having a generally small reinforcing effect over northern Africa, and a balancing effect elsewhere. Therefore, despite the large uncertainties in projected changes in the diurnal temperature range, the reduction of tropical climate land area is a robust response to global warming, associated primarily with increased seasonal temperature range in the tropics.

Since the increased seasonal temperature range is associated with reduced evaporative cooling during summer (Chen et al., 2019; Sobel & Camargo, 2011), we examine the ensemble-mean changes in summer precipitation minus evaporation ($P - E$), as well as precipitation and evaporation individually, normalized per 1K global warming, in Figure 5. Along the edges of tropical climate land areas (magenta lines in Figures 4 and 5), while there is no appreciable net drying (i.e., change in $P - E$), increased Δ_{Seasonal} goes along with increased evaporation during southern and northern hemisphere summers (left and right panels, respectively) over northern Africa, Asia, and South America. The increased evaporation over northern Africa and Asia persists year round and may also account for the increased Δ_{Diurnal} there as well. These results are generally consistent with the projected increased

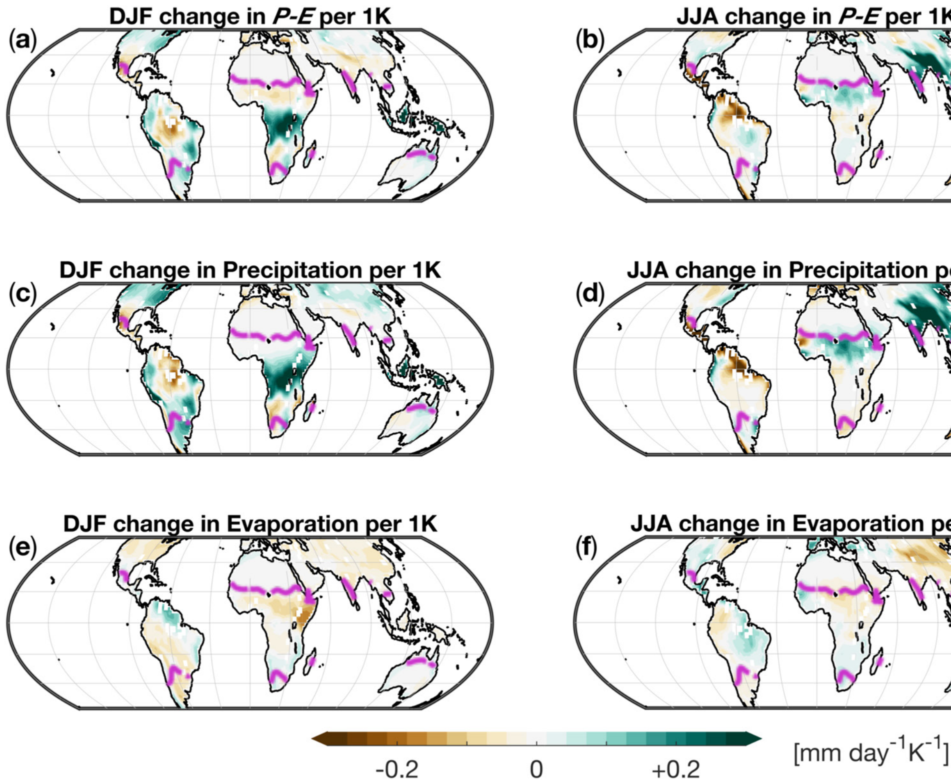

Figure 5. CMIP5/6 ensemble mean projected changes over land per 1K global mean temperature warming during December–February (left panels) and June–August (right panels) of (a, b) precipitation minus evaporation ($P - E$), (c, d) precipitation, and (e, f) evaporation. Magenta lines show latitudes where $\Delta_{\mathrm{Diurnal}} - \Delta_{\mathrm{Seasonal}} = 0$.

aridity over land, especially in subtropical regions, caused by a greater rate of increase by potential evapotranspiration relative to precipitation in a warming climate (Chai et al., 2021; Feng & Fu, 2013; Fu & Feng, 2014; Sherwood & Fu, 2014). Thus, we hypothesize that reduced evaporative cooling in the subtropics is a key driver of the reduced tropical climate land area.

4. Summary and Discussion

Tropical climate land areas can be defined as regions where the diurnal surface temperature range exceeds the seasonal surface temperature range (Figure 1). Based on this definition we find a robust reduction of tropical land area with global warming in a cohort of 27 CMIP5 and 18 CMIP6 models forced with high-emission scenarios.

The projected decrease in tropical land area is driven primarily by an increased seasonal temperature range (Figure 2b), consistently seen across regions (Figure 4b), caused by enhanced summer warming (Figure 5; Sobel & Camargo, 2011; Chen et al., 2019). The diurnal temperature range generally decreases in the northern hemisphere and increases in the southern hemisphere (Figure 2b), and has an overall small contribution to the changes in tropical land area (Figure 4c). Thus, despite large uncertainties in simulated trends of the diurnal temperature range, the reduction of tropical land area with global warming is a robust response, seen in nearly all of the CMIP5/6 models (Figures 3a and 3b).

The net loss of tropical land area with global warming is consistent with the projected equatorward and poleward expansion of the SDZs (Figure 3d; Lau & Kim, 2015; Lu et al., 2007), as well as with the narrowing of the TRB (Figure 3e; Byrne & Schneider, 2016b). However, a narrowing of the TRB is not seen over land. Thus, the reduced extent of tropical climate land areas is not clearly linked to these trends, which are associated with changes in the mean meridional circulation (MOC; Byrne & Schneider, 2016b; Lu et al., 2007; Staten et al., 2020). Moreover, the term "Tropical widening" commonly used to describe the expansion of the tropical MOC (Seidel et al., 2008; Staten et al., 2020) is revealed here to be ambiguous. Given the equatorward and poleward expansion of the SDZs

(Figure 3d), the term "Subtropical widening" would be a more appropriate descriptor, consistent with the reduction of tropical climate land area in a warming climate.

Consistent with previous studies, we hypothesize that reduced evaporative cooling during summer may account for changes in the seasonal temperature ranges over northern Africa, Asia and south America (Chen et al., 2019; Sobel & Camargo, 2011). Changes in the diurnal temperature range over northern Africa and Asia likewise agree with increased evaporation there (Figures 4 and 5). These results suggest that the general tendency toward more arid conditions under global warming is a key driver for the reduced tropical land area, which is of critical importance to populations living along the transition regions such as the Sahel, the eastern Mediterranean, and southeast Asia (Carvalho et al., 2022; Chai et al., 2021; D'Agostino & Lionello, 2020; Fu & Feng, 2014; Sherwood & Fu, 2014). However, a complete surface energy budget analysis is required to fully reveal the drivers of seasonal and diurnal temperature ranges. Further analysis is also required to better understand the regional causes and implications of reduced tropical land area, especially in regions where evaporation or aridity are not projected to increase (Figure 5; Huang et al., 2017; Sherwood & Fu, 2014).

Appendix A: Width of the Tropical Rain Belt

Defining the centroid latitude of the meridional distribution of zonal-mean precipitation P as

$$\phi_{cent} = \int_{20^\circ S}^{20^\circ N} P(\phi)\phi\cos(\phi)\mathrm{d}\phi, \tag{A1}$$

the width of the TRB is estimated as the standard deviation of the meridional precipitation distribution,

$$\mathrm{W}_{TRB} = \left[\frac{\int_{20^\circ S}^{20^\circ N} P(\phi)(\phi - \phi_{cent})^2\cos(\phi)\mathrm{d}\phi}{\int_{20^\circ S}^{20^\circ N} P(\phi)\cos(\phi)\mathrm{d}\phi}\right]^{\frac{1}{2}}. \tag{A2}$$

This width estimate is generally well correlated with other TRB width indices across CMIP5/6 models (Adam et al., 2023), and can be consistently applied to global and over-land zonal averages of precipitation. Results based on this estimate are also not statistically different (at 95% confidence) from those obtained using TRB width defined as the difference between the northern and southern hemisphere precipitation centroids, used by Donohoe et al. (2019). Other indices of TRB width which rely on the meridional mass streamfunction or geometric quantities of the precipitation distribution (Byrne et al., 2018; Popp & Lutsko, 2017) cannot be applied over land due to the irregular regional precipitation distributions.

Data Availability Statement

All of the data used in the analyses presented here is publicly available. We thank the climate modeling groups for producing and making available their model output, the Earth System Grid Federation (ESGF) for archiving the data and providing access, and the multiple funding agencies who support CMIP and ESGF. All CMIP data analyzed here are available from the ESGF at https://esgf-node.llnl.gov/projects/esgf-llnl. The CMIP5 and CMIP6 models used can be found in Table S1 in Supporting Information S1.

Acknowledgments
OA acknowledges support by ISF Grant 1022/21. We thank the two anonymous reviewers for their helpful suggestions.

References

Adam, O., Farnsworth, A., & Lunt, D. J. (2023). Modality of the tropical rain belt across models and simulated climates. *Journal of Climate*, *36*(5), 1331–1345.

Adam, O., Grise, K. M., Staten, P., Simpson, I. R., Davis, S. M., Davis, N. A., et al. (2018). The TropD software package (v1): Standardized methods for calculating tropical-width diagnostics. *Geoscientific Model Development*, *11*(10), 4339–4357. https://doi.org/10.5194/gmd-11-4339-2018

Adam, O., Schneider, T., & Harnik, N. (2014). Role of changes in mean temperatures versus temperature gradients in the recent widening of the Hadley circulation. *Journal of Climate*, *27*(19), 7450–7461. https://doi.org/10.1175/jcli-d-14-00140.1

Barlow, J., França, F., Gardner, T. A., Hicks, C. C., Lennox, G. D., Berenguer, E., et al. (2018). The future of hyperdiverse tropical ecosystems. *Nature*, *559*(7715), 517–526. https://doi.org/10.1038/s41586-018-0301-1

Byrne, M. P., Pendergrass, A. G., Rapp, A. D., & Wodzicki, K. R. (2018). Response of the intertropical convergence zone to climate change: Location, width, and strength. *Current Climate Change Reports*, *4*(4), 355–370. https://doi.org/10.1007/s40641-018-0110-5

Byrne, M. P., & Schneider, T. (2016a). Energetic constraints on the width of the intertropical convergence zone. *Journal of Climate*, *29*(13), 4709–4721. https://doi.org/10.1175/jcli-d-15-0767.1

Byrne, M. P., & Schneider, T. (2016b). Narrowing of the ITCZ in a warming climate: Physical mechanisms. *Geophysical Research Letters*, *43*(21), 11–350. https://doi.org/10.1002/2016gl070396

Carvalho, D., Pereira, S., Silva, R., & Rocha, A. (2022). Aridity and desertification in the Mediterranean under EURO-CORDEX future climate change scenarios. *Climatic Change*, *174*(3–4), 28. https://doi.org/10.1007/s10584-022-03454-4

Chai, R., Mao, J., Chen, H., Wang, Y., Shi, X., Jin, M., et al. (2021). Human-caused long-term changes in global aridity. *npj Climate and Atmospheric Science*, *4*(1), 65. https://doi.org/10.1038/s41612-021-00223-5

Chen, J., Dai, A., & Zhang, Y. (2019). Projected changes in daily variability and seasonal cycle of near-surface air temperature over the globe during the twenty-first century. *Journal of Climate*, *32*(24), 8537–8561. https://doi.org/10.1175/jcli-d-19-0438.1

D'Agostino, R., & Lionello, P. (2020). The atmospheric moisture budget in the Mediterranean: Mechanisms for seasonal changes in the Last Glacial Maximum and future warming scenario. *Quaternary Science Reviews*, *241*, 106392. https://doi.org/10.1016/j.quascirev.2020.106392

Dai, A., Genio, A. D. D., & Fung, I. Y. (1997). Clouds, precipitation and temperature range. *Nature*, *386*(6626), 665–666. https://doi.org/10.1038/386665b0

Donohoe, A., Atwood, A. R., & Byrne, M. P. (2019). Controls on the width of tropical precipitation and its contraction under global warming. *Geophysical Research Letters*, *46*(16), 9958–9967. https://doi.org/10.1029/2019gl082969

Donohoe, A., & Battisti, D. S. (2013). The seasonal cycle of atmospheric heating and temperature. *Journal of Climate*, *26*(14), 4962–4980. https://doi.org/10.1175/jcli-d-12-00713.1

Dwyer, J. G., Biasutti, M., & Sobel, A. H. (2012). Projected changes in the seasonal cycle of surface temperature. *Journal of Climate*, *25*(18), 6359–6374. https://doi.org/10.1175/jcli-d-11-00741.1

Eyring, V., Bony, S., Meehl, G. A., Senior, C. A., Stevens, B., Stouffer, R. J., & Taylor, K. E. (2016). Overview of the Coupled Model Intercomparison Project Phase 6 (CMIP 6) experimental design and organization. *Geoscientific Model Development*, *9*(5), 1937–1958. https://doi.org/10.5194/gmd-9-1937-2016

Feng, S., & Fu, Q. (2013). Expansion of global drylands under a warming climate. *Atmospheric Chemistry and Physics*, *13*(19), 10081–10094. https://doi.org/10.5194/acp-13-10081-2013

Fiedler, S., Crueger, T., D'Agostino, R., Peters, K., Becker, T., Leutwyler, D., et al. (2020). Simulated tropical precipitation assessed across three major phases of the Coupled Model Intercomparison Oroject (CMIP). *Monthly Weather Review*, *148*(9), 3653–3680. https://doi.org/10.1175/mwr-d-19-0404.1

Fu, Q., & Feng, S. (2014). Responses of terrestrial aridity to global warming. *Journal of Geophysical Research: Atmospheres*, *119*(13), 7863–7875. https://doi.org/10.1002/2014jd021608

Garfinkel, C. I., Adam, O., Morin, E., Enzel, Y., Elbaum, E., Bartov, M., et al. (2020). The role of zonally averaged climate change in contributing to intermodel spread in CMIP5 predicted local precipitation changes. *Journal of Climate*, *33*(3), 1141–1154. https://doi.org/10.1175/jcli-d-19-0232.1

Gaston, K. J. (2000). Global patterns in biodiversity. *Nature*, *405*(6783), 220–227. https://doi.org/10.1038/35012228

Geerts, B. (2003). Empirical estimation of the monthly-mean daily temperature range. *Theoretical and Applied Climatology*, *74*(3), 145–165. https://doi.org/10.1007/s00704-002-0715-3

Gelaro, R., McCarty, W., Suárez, M. J., Todling, R., Molod, A., Takacs, L., et al. (2017). The modern-era retrospective analysis for research and applications, version 2 (MERRA-2). *Journal of Climate*, *30*(14), 5419–5454. https://doi.org/10.1175/jcli-d-16-0758.1

Grünzweig, J. M., De Boeck, H. J., Rey, A., Santos, M. J., Adam, O., Bahn, M., et al. (2022). Dryland mechanisms could widely control ecosystem functioning in a drier and warmer world. *Nature Ecology & Evolution*, *6*(8), 1–13. https://doi.org/10.1038/s41559-022-01779-y

He, J., & Soden, B. J. (2017). A re-examination of the projected subtropical precipitation decline. *Nature Climate Change*, *7*(1), 53–57. https://doi.org/10.1038/nclimate3157

Hersbach, H., Bell, B., Berrisford, P., Hirahara, S., Horányi, A., Muñoz-Sabater, J., et al. (2020). The era5 global reanalysis. *Quarterly Journal of the Royal Meteorological Society*, *146*(730), 1999–2049. https://doi.org/10.1002/qj.3803

Holmes, C. R., Woollings, T., Hawkins, E., & De Vries, H. (2016). Robust future changes in temperature variability under greenhouse gas forcing and the relationship with thermal advection. *Journal of Climate*, *29*(6), 2221–2236. https://doi.org/10.1175/jcli-d-14-00735.1

Huang, J., Li, Y., Fu, C., Chen, F., Fu, Q., Dai, A., et al. (2017). Dryland climate change: Recent progress and challenges. *Reviews of Geophysics*, *55*(3), 719–778. https://doi.org/10.1002/2016rg000550

Lau, W. K., & Kim, K.-M. (2015). Robust Hadley Circulation changes and increasing global dryness due to CO_2 warming from CMIP5 model projections. *Proceedings of the National Academy of Sciences*, *112*(12), 3630–3635. https://doi.org/10.1073/pnas.1418682112

Lehner, F., & Stocker, T. F. (2015). From local perception to global perspective. *Nature Climate Change*, *5*(8), 731–734. https://doi.org/10.1038/nclimate2660

Liu, Y., Cai, W., Lin, X., & Li, Z. (2022). Increased extreme swings of Atlantic intertropical convergence zone in a warming climate. *Nature Climate Change*, *12*(9), 828–833. https://doi.org/10.1038/s41558-022-01445-y

Lu, J., Vecchi, G. A., & Reichler, T. (2007). Expansion of the Hadley cell under global warming. *Geophysical Research Letters*, *34*(6), L06805. https://doi.org/10.1029/2006GL028443

Mamalakis, A., Randerson, J. T., Yu, J.-Y., Pritchard, M. S., Magnusdottir, G., Smyth, P., et al. (2021). Zonally contrasting shifts of the tropical rain belt in response to climate change. *Nature Climate Change*, *11*(2), 143–151. https://doi.org/10.1038/s41558-020-00963-x

Manabe, S., Ploshay, J., & Lau, N.-C. (2011). Seasonal variation of surface temperature change during the last several decades. *Journal of Climate*, *24*(15), 3817–3821. https://doi.org/10.1175/jcli-d-11-00129.1

Nguyen, H., Evans, A., Lucas, C., Smith, I., & Timbal, B. (2013). The Hadley circulation in reanalyses: Climatology, variability, and change. *Journal of Climate*, *26*(10), 3357–3376. https://doi.org/10.1175/jcli-d-12-00224.1

Paffen, K. (1967). Das verhältnis der Tages-zur jahreszeitlichen Temperaturschwankung: Erläuterungen zu einer neuen Weltkarte als Beitrag zur allgemeinen Klimageographie (the relationship of diurnal to annual temperature variations). *Erdkunde*, *XXI*, 94–111.

Pekel, J.-F., Cottam, A., Gorelick, N., & Belward, A. S. (2016). High-resolution mapping of global surface water and its long-term changes. *Nature*, *540*(7633), 418–422. https://doi.org/10.1038/nature20584

Popp, M., & Lutsko, N. (2017). Quantifying the zonal-mean structure of tropical precipitation. *Geophysical Research Letters*, *44*(18), 9470–9478. https://doi.org/10.1002/2017gl075235

Riehl, H. (1954). *Tropical meteorology* (Technical report). McGraw-Hill.

Riehl, H. (1979). *Climate and weather in the tropics*. Academic Press.

Ruane, A., Ranasinghe, R., Vautard, R., Arnell, N., Coppola, E., Cruz, F. A., et al. (2021). IPCC AR6 WGI Chapter 12: Climate change information for regional impact and for risk assessment. In *Agu fall meeting abstracts* (Vol. 2021, p. U13B–12).

Schmidt, D. F., & Grise, K. M. (2017). The response of local precipitation and sea level pressure to Hadley cell expansion. *Geophysical Research Letters*, *44*(20), 10–573. https://doi.org/10.1002/2017gl075380

Seager, R., Liu, H., Henderson, N., Simpson, I., Kelley, C., Shaw, T., et al. (2014). Causes of increasing aridification of the Mediterranean region in response to rising greenhouse gases. *Journal of Climate*, *27*(12), 4655–4676. https://doi.org/10.1175/jcli-d-13-00446.1

Seager, R., Naik, N., & Vecchi, G. A. (2010). Thermodynamic and dynamic mechanisms for large-scale changes in the hydrological cycle in response to global warming. *Journal of Climate*, *23*(17), 4651–4668. https://doi.org/10.1175/2010jcli3655.1

Seidel, D. J., Fu, Q., Randel, W. J., & Reichler, T. J. (2008). Widening of the tropical belt in a changing climate. *Nature Geoscience*, *1*, 21–24. https://doi.org/10.1038/ngeo.2007.38

Seviour, W. J., Davis, S. M., Grise, K. M., & Waugh, D. W. (2018). Large uncertainty in the relative rates of dynamical and hydrological tropical expansion. *Geophysical Research Letters*, *45*(2), 1106–1113. https://doi.org/10.1002/2017gl076335

Sherwood, S., & Fu, Q. (2014). A drier future? *Science*, *343*(6172), 737–739. https://doi.org/10.1126/science.1247620

Si, D., Ding, Y., & Liu, Y. (2009). Decadal northward shift of the Meiyu belt and the possible cause. *Chinese Science Bulletin*, *54*(24), 4742–4748. https://doi.org/10.1007/s11434-009-0385-y

Sobel, A. H., & Camargo, S. J. (2011). Projected future seasonal changes in tropical summer climate. *Journal of Climate*, *24*(2), 473–487. https://doi.org/10.1175/2010jcli3748.1

Staten, P. W., Grise, K. M., Davis, S. M., Karnauskas, K. B., Waugh, D. W., Maycock, A. C., et al. (2020). Tropical widening: From global variations to regional impacts. *Bulletin of the American Meteorological Society*, *101*(6), E897–E904. https://doi.org/10.1175/BAMS-D-19-0047.1

Staten, P. W., Lu, J., Grise, K. M., Davis, S. M., & Birner, T. (2018). Re-examining tropical expansion. *Nature Climate Change*, *8*(9), 768–775. https://doi.org/10.1038/s41558-018-0246-2

Stine, A. R., & Huybers, P. (2012). Changes in the seasonal cycle of temperature and atmospheric circulation. *Journal of Climate*, *25*(21), 7362–7380. https://doi.org/10.1175/jcli-d-11-00470.1

Stouffer, R., & Wetherald, R. (2007). Changes of variability in response to increasing greenhouse gases. Part I: Temperature. *Journal of Climate*, *20*(21), 5455–5467. https://doi.org/10.1175/2007jcli1384.1

Taylor, K. E., Stouffer, R. J., & Meehl, G. A. (2012). An overview of CMIP5 and the experiment design. *Bulletin of the American Meteorological Society*, *93*(4), 485–498. https://doi.org/10.1175/bams-d-11-00094.1

Thorne, P., Donat, M., Dunn, R., Williams, C., Alexander, L., Caesar, J., et al. (2016). Reassessing changes in diurnal temperature range: Intercomparison and evaluation of existing global data set estimates. *Journal of Geophysical Research: Atmospheres*, *121*(10), 5138–5158. https://doi.org/10.1002/2015jd024584

Thorne, P., Menne, M., Williams, C., Rennie, J., Lawrimore, J., Vose, R., et al. (2016). Reassessing changes in diurnal temperature range: A new data set and characterization of data biases. *Journal of Geophysical Research: Atmospheres*, *121*(10), 5115–5137. https://doi.org/10.1002/2015jd024583

Troll, C. (1943). Thermische klimatypen der Erde (thermal climate types of Earth). *Petermanns Geographische Mitteilungen*, *43*(3/4), 81–89.

Tuel, A., O'Gorman, P. A., & Eltahir, E. A. (2021). Elements of the dynamical response to climate change over the Mediterranean. *Journal of Climate*, *34*(3), 1135–1146. https://doi.org/10.1175/jcli-d-20-0429.1

Wang, B., Biasutti, M., Byrne, M. P., Castro, C., Chang, C.-P., Cook, K., et al. (2021). Monsoons climate change assessment. *Bulletin of the American Meteorological Society*, *102*(1), E1–E19. https://doi.org/10.1175/bams-d-19-0335.1

Wang, C., Zhang, L., Lee, S.-K., Wu, L., & Mechoso, C. R. (2014). A global perspective on CMIP5 climate model biases. *Nature Climate Change*, *4*(3), 201–205. https://doi.org/10.1038/nclimate2118

Wang, K., & Clow, G. D. (2020). The diurnal temperature range in CMIP6 models: Climatology, variability, and evolution. *Journal of Climate*, *33*(19), 8261–8279. https://doi.org/10.1175/jcli-d-19-0897.1

Warszawski, L., Frieler, K., Huber, V., Piontek, F., Serdeczny, O., Zhang, X., et al. (2017). Center for international earth science information network—CIESIN—Columbia University. (2016). Gridded population of the world, version 4 (GPWv4): Population density. Palisades. In *Atlas of environmental risks facing China under climate change* (p. 228). NASA Socioeconomic Data and Applications Center (SEDAC). https://doi.org/10.7927/h4np22dq

Waugh, D., Grise, K. M., Seviour, W., Davis, S., Davis, N., Adam, O., et al. (2018). Revisiting the relationship among metrics of tropical expansion. *Journal of Climate*, *31*, 7565–7581. https://doi.org/10.1175/JCLI-D-18-0108.1

Wild, M. (2009). Global dimming and brightening: A review. *Journal of Geophysical Research*, *114*(D10), D00D16. https://doi.org/10.1029/2008jd011470

Yang, G.-Y., & Slingo, J. (2001). The diurnal cycle in the tropics. *Monthly Weather Review*, *129*(4), 784–801. https://doi.org/10.1175/1520-0493(2001)129<0784:tdcitt>2.0.co;2

Yettella, V., & England, M. R. (2018). The role of internal variability in twenty-first-century projections of the seasonal cycle of northern hemisphere surface temperature. *Journal of Geophysical Research: Atmospheres*, *123*(23), 13–149. https://doi.org/10.1029/2018jd029066

Yin, J., & Porporato, A. (2017). Diurnal cloud cycle biases in climate models. *Nature Communications*, *8*(1), 2269. https://doi.org/10.1038/s41467-017-02369-4